

Controls on the recycling and preservation of biogenic silica from biomineralization to burial

Socratis Loucaides (corresponding author)

National Oceanography Centre, University of Southampton, Southampton, UK

Email: s.loucaides@noc.soton.ac.uk

TEL: +44 (0) 2380593641

Philippe Van Cappellen

School of Earth and Atmospheric Sciences, Georgia Institute of Technology, Atlanta, Georgia, USA

Vincent Roubéix

Cemagref, UR REBX, F-33612 Cestas Cedex, France

Brivaela Moriceau

Institut Universitaire Européen de la Mer, UMR CNRS 6539, Plouzané, France

Olivier Ragueneau

Institut Universitaire Européen de la Mer, UMR CNRS 6539, Plouzané, France

Keywords : Biogenic silica, dissolution, diagenesis, silicon cycle, biomineralization

Abstract

The recycling of biogenic silica (bSiO₂) produced by diatoms is a vital process sustaining a significant fraction of primary production in the oceans. The efficiency with which bSiO₂ dissolves controls the availability of nutrient silicon in the water column, and modulates the export of organic carbon to the deep sea. Environmental conditions during biomineralization (temperature, nutrient availability, light, etc.) affect the silicification and weathering resistance of diatom frustules, while ecosystem processes, including grazing and aggregation, are determining factors for the recycling of bSiO₂ in the water column. Bacterial colonization of dead diatoms leads to the decomposition of the protective organic layers allowing for the dissolution of bSiO₂ to begin.

The dissolution rate of diatom frustules is a function of the physicochemical properties of both the silica (e.g., specific surface area, degree of hydration and condensation, impurities) and the aqueous medium (e.g., temperature, pH, pressure, electrolyte composition). In sediments, the dissolution of bSiO₂ is controlled by the presence of lithogenic minerals, aging processes and the build up of dSi in the pore waters. In particular, interactions between lithogenic silicate minerals and bSiO₂ may initiate rapid diagenetic alterations that favor the preservation of bSiO₂.

1. The oceanic Si cycle

The recycling of biogenic silica (bSiO₂) is a key biogeochemical process controlling the availability of nutrient Si in the global ocean [1-3]. Dissolved silicate (dSi) sustains a significant fraction of the oceanic primary production, which is carried out by diatoms [4]. Because of the close coupling between the Si and C cycles, substantial research has been conducted during the last few decades in order to better understand the biogeochemical cycling of Si in both aquatic and terrestrial environments [2, 5, 6].

The coupling of the marine Si and C cycles, however, is not a simple one. Rates of primary and biosiliceous productivity do not always match opal accumulation rates in the underlying sediments [7]. For example, high rates of opal accumulation are observed in the Southern Ocean, despite relatively low biosiliceous and carbon production in the region. In comparison, high bSiO₂ productivity in the Northern Atlantic is accompanied by almost no opal preservation in the sediments. This phenomenon, commonly referred to as the “opal paradox”, indicates that the recycling efficiency of bSiO₂ exhibits significant spatial and temporal variability [4]. Variable bSiO₂ preservation efficiencies present a

major obstacle when reconstructing past environmental conditions using sedimentary records [2, 8-14].

Field studies and laboratory experiments have greatly advanced our understanding of how ecosystem processes, material properties and environmental conditions affect the recycling and preservation of bSiO_2 in the oceans and in terrestrial environments. The purpose of this paper is to review some key facts about bSiO_2 dissolution in natural environments. Emphasis will be given to the dissolution of diatom frustules in the water column and the sediments of the ocean (Fig.1).

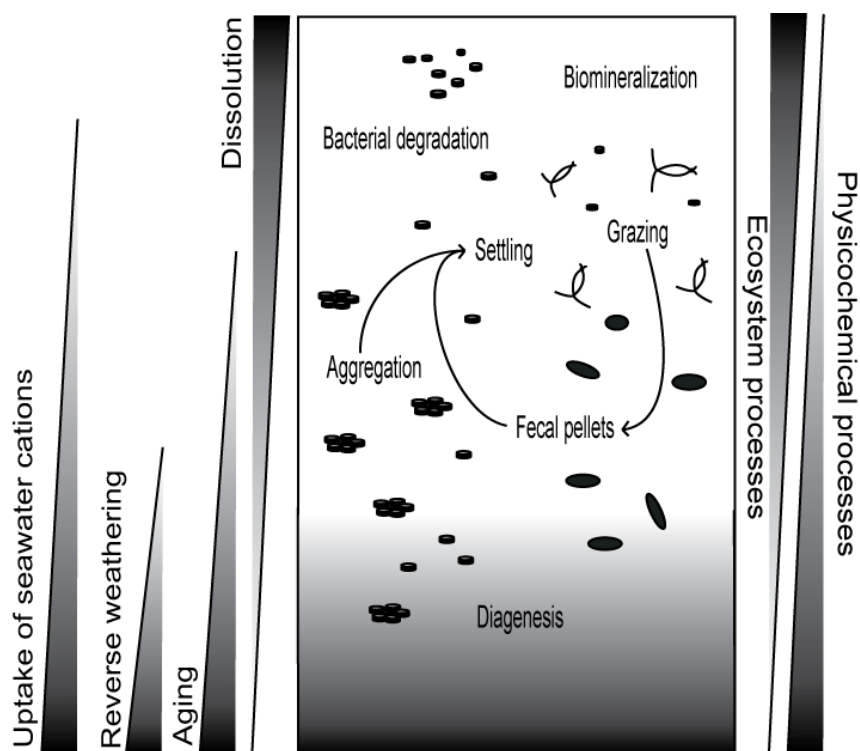


Fig. 1 Schematic of the physicochemical and ecosystem processes that control the recycling efficiency of bSiO_2 from the surface waters to the bottom sediments. Several ecosystem processes are predominant in the upper water column while physicochemical forcings prevail in the sediments through the interaction of bSiO_2 with other mineral phases

2. Biomineralization and the weathering resistance of diatom frustules

2.1 Cell growth and silicification

The rate at which bSiO_2 dissolves is in a large measure dependent on the intrinsic physicochemical properties of the amorphous silica material produced during biosynthesis. Genetic variations in diatom frustule silicification and morphology help explain the large variability in dissolution efficiency between different diatom species. Laboratory dissolution experiments have shown that the half life of diatom frustule counts (i.e. the time required for the number of frustules of a given species to decline by 50%) can vary by up to 30 orders of magnitude between different taxa [10]. Significant variations in frustule silicification are also common within the same diatom species. Studies indicate that the degree of silicification is a function of the cellular growth rate, and the ambient dSi concentration during biosynthesis [15]. While during periods of Si limitation diatoms are able to maintain their division rates [16-18], they are forced to build less silicified frustules ([15] and references therein). When Si is not limited, however, the degree of silicification is mainly a function of the cellular growth rate. Longer cell cycles during slow growth, allow for maximum uptake of dSi by diatoms while the contrary occurs during rapid growth.

Claquin et al. [19] monitored the growth rates and bSiO_2 content of diatoms (*Thalassiosira pseudonana*) cultured under light, nitrogen, and phosphorous limitation. They observed that the bSiO_2 content of the cells decreased with increasing growth rates (Fig. 2), while the volume of the cells remained practically constant. Their results confirm that faster growth rates force diatoms to built thinner frustules. The growth rate of diatoms is a function of several environmental parameters, including light intensity [20, 21], temperature [22, 23], and nutrient availability [15, 24, 25], therefore, these parameters indirectly control the silicification and weathering resistance of diatom frustules.

Marine environments tend to be more Si-limited than continental aquatic ecosystems. This may be one reason why marine diatoms exhibit up to one order of magnitude less silica mass per cell than freshwater diatoms, although different adaptation

mechanisms between freshwater and marine species may also play a role [26]. Less silicified marine diatoms have higher buoyancy allowing them to stay longer in the photic zone. Sinking below the photic zone can be a fatal journey for marine diatoms, but in lacustrine environments resuspension and vertical mixing can lift the diatoms back to the photic zone after sinking into the hypolimnion. River environments are also more energetic, so positive buoyancy may not be as critical.

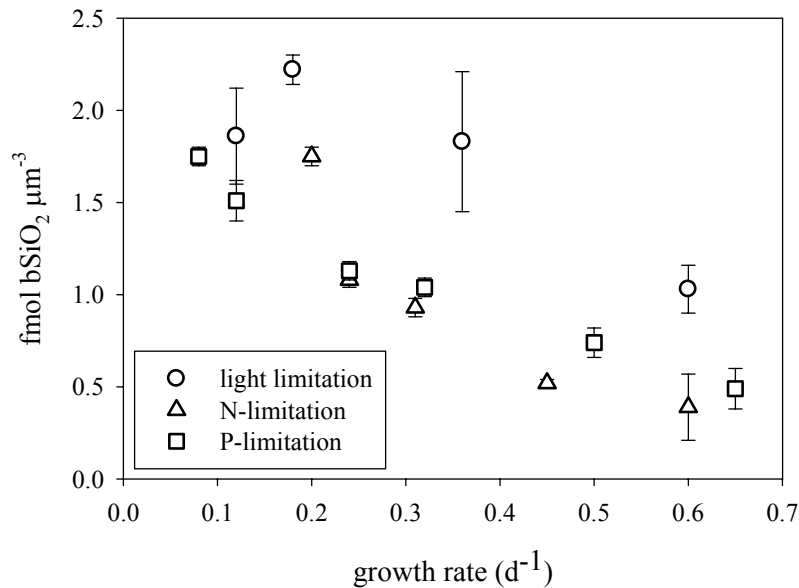


Fig. 2 Change in the cellular bSiO₂ content of cultured diatoms (*Thalassiosira pseudonana*), normalized by cell volume, as a function of growth rate. The y-axis ultimately represents the thickness of the diatom frustules which decreases at faster growth rates. The diatoms were cultured under either light, nitrogen, or phosphorous limitation (Data from Claquin et al. [19])

Recent evidence suggests that growth rate and dSi availability may not be the only factors controlling the silicification of diatom frustules. Pondaven et al. [27] demonstrated that diatoms cultured together with herbivores produced more silicified frustules than diatoms grown alone. Their observations suggest that grazing-induced increase in silicification represents an adaptive reaction to grazing, and that silicification in diatoms is also a phenotypically plastic trait modulated by grazing pressure.

The dissolution rate of diatom frustules free from organic coatings is directly proportional to the surface area of the interface between the bSiO₂ and the solvent

(water). The shape, weight, and morphology of a diatom frustule, define its specific surface area (SSA), which is equal to the ratio between the surface area and mass of the frustule. The SSA can also be a measure of the degree of silicification of diatom frustules. For a dissolving diatom frustule this property determines its recycling efficiency. For instance, diatom frustules of identical mass dissolve in rates that are proportional to their surface area [28]. Therefore, frustules with low specific surface area generally sink deeper into the water column before they completely dissolve.

Because of their complex surface morphology, diatom frustules are characterized by relatively large specific surface areas that can vary between species by as much as one order of magnitude, typically between 20 to 200 m² g⁻¹ [29, 30]. Due to the intricate surface morphology of diatom frustules, their true exposed surface area (as measured by gas absorption techniques) can often be orders of magnitude larger than the geometric surface area derived from the size of the frustule [30]. Although evidence suggests that the geometric surface area of diatom frustules may vary depending on growth conditions [15, 19, 31], there is still a lack of knowledge on how the “true” surface area is affected. Spectroscopic evidence, however, suggest that the shape and size of micropores in diatom frustules is influenced by environmental conditions during biomineralization [32].

The production of less silicified frustules during non-limiting conditions has a negative impact on the bSiO₂ export but also the carbon export to the deep ocean. Diatoms grown during limiting conditions are more effective silicon and carbon exporters, and tend to predominate in the sedimentary record [33-35]. On the contrary, the export of carbon during non-limiting conditions (i.e. algal blooms) may not be as significant as previously thought, because the bSiO₂ and organic carbon are efficiently recycled within the upper ocean.

2.2 Aluminum incorporation during biomineralization

Diatoms may provide an important link between the marine silicon and aluminum cycles, by controlling the availability of dissolved Al in the surface ocean [36]. Although the exact role Al plays in the biological functioning of diatoms remains unclear, the assimilation of Al by diatoms seems to affect the development of diatom communities, as

well as the physiology of individual cells [32, 37-39]. Culture studies show that Al has a limiting effect on the dSi assimilation by diatoms, although it has no effect on their division rates [38]. This suggests that Al availability enhances the silicification of diatom frustules [39] without, however, affecting their growth rates.

Aluminum incorporation into amorphous silica is known to reduce silica solubility and dissolution rates [28, 40]. However, even when diatoms are grown in Al-rich media the Al content of the diatom frustules does not exceed 0.8% [41, 42]. In marine waters where Al concentrations are generally low ($<0.1\mu\text{M}$) Al:Si atomic ratios of diatom frustules remain well below 10^{-4} [43]. These levels are generally too low to significantly affect dissolution kinetics or the solubility of diatom frustules [28].

3 Early post-mortem processes: Si - C interactions

3.1 Organic coatings and bacteria

During the lifetime of a diatom, its frustule resists dissolution due to the presence of an external organic coating composed mainly of proteins and structural carbohydrates [44]. The protective role of the organic coating has been demonstrated experimentally. Diatom frustules, from which the organic matter has been removed, dissolve faster than frustules with the organic layer intact [45-47]. After diatoms die, the organic layer is decomposed by bacteria and dissolution of the exposed silica can no longer be avoided [45, 48].

Bacteria decompose the organic matter of diatom cells by producing proteases. The importance of bacterial proteases for the dissolution of fresh diatoms has been well documented [49]. It has been shown that the dissolution of diatom detritus was faster after addition of bacterial proteases under axenic conditions, and strongly reduced by the addition of protease inhibitors in the presence of bacteria. Moreover during the biodegradation of diatom detritus by bacteria, the bacterial ectoprotease activity was highest, compared to other enzymatic activity, and it correlated with the bSiO_2 dissolution rates. Particularly during the first days of diatom biodegradation, protease were found most active in detaching serin and glycin residues, the two most abundant amino acids in the organic coatings of diatoms [44]. Dense colonization by bacteria of the

surface of diatom frustules may lead to the formation of microenvironments characterized by high concentrations of bacterial ectoenzymes which increase the decomposition of the organic coatings [49].

The impact of bacteria on bSiO_2 dissolution likely depends on the nature of the bacterial community present in close proximity to the diatom cells, and on the environmental conditions controlling bacterial activity (e.g. temperature [50], pressure [51] and nutrient availability [52]). Species composition, ectoprotease profile, colonization dynamics, and the aggregating effect on diatom detritus are all ways by which the bacterial assemblage can modulate bSiO_2 dissolution [45]. In addition, the effects of various metabolic products accumulating in the bacterial microenvironment around diatom frustules on the dissolution of bSiO_2 still remain to be fully characterized [53].

3.2 Aggregation

Although aggregation seems to occur mainly under nutrient limiting conditions [54, 55], the processes controlling diatom aggregation are yet to be fully unraveled. What seems clear, however, is that diatoms can excrete polysaccharides that, after partial dissolution, become so-called transparent exopolymer particles (TEP) [56, 57]. This gel-like substance favors the cohesion between diatom cells after they collide, which then triggers diatom aggregation. Experimental observations indicate that grazing pressure [58], nutrient availability [54, 55], light intensity [59], and the presence of bacteria [60], affect TEP concentrations and adhesivity, which in turn control aggregation rates.

Aggregation influences the balance between recycling and preservation of bSiO_2 as aggregated diatoms sink faster [61, 62] than free suspended cells, leaving less time for dissolution. Furthermore, diatoms in aggregates also dissolve slower than free suspended cells [63]. The decrease of the dissolution rate is due in part to the higher internal dSi concentrations inside the aggregates, but also to the higher proportion of diatom cells that remain alive in the aggregates. Other factors could play a role in retarding dissolution. For example, the pH inside aggregates has been shown to be lower (pH \sim 7) than typical seawater pH, possibly due to the respiratory activity of diatoms and bacteria [64].

Bacterial densities and activities can also be higher in aggregates [65, 66]. Degradation of the organic coatings of diatom cells could then be controlled by the relative nutritional values of TEP and coatings to the bacteria.

3.3 Grazing and fecal pellets

Diatoms are at the basis of the oceanic food web, and the most important food source for zooplankton. For diatoms, the silica frustule does not only provide support and rigidity to the cells but also provides some protection against small grazers [67]. Even though once ingested most diatom frustules break, some remain intact even when the internal carbon has been digested [68], while some diatoms can even make it out of zooplankton guts alive [69, 70].

Zooplankton fecal pellets can sink at rates of up to 2000-3000 m d⁻¹ [68]. Contrarily to aggregates, fecal pellets are very robust particles that cannot be easily destroyed. When diatoms are embedded into large fecal pellets they are essentially protected from dissolution mainly due to reduced contact between the bSiO₂ and seawater. Dissolution rates of bSiO₂ inside fecal pellets can be 2 to 10 times lower than dissolution rates of freely suspended diatoms [71]. Fecal pellets, however, are also subject to grazing by coprophages who can destroy the pellets and retrieve the broken diatom frustules. In that case the bSiO₂ dissolution rate increases [71].

Grazing of freely suspended diatoms and aggregates also takes place at the bottom of shallow marine ecosystems by benthic organisms such as filter feeders. Silica dissolution rates measured in feces of the benthic filter feeder *Crepidula fornicata* show that bSiO₂ is protected from dissolution by the peritrophic membrane of the fecal pellets [Moriceau, unpublished]. When the fecal pellets are destroyed the silica dissolution rates increase, because of the presence of broken frustules (and thus higher exposed surface areas) in the pellets [63].

4 Geochemical water column processes

4.1 Theoretical background

The process of silica dissolution, being of great interest to both material scientists and geochemists, has been studied extensively [40, 72-75]. It is generally accepted that the dissolution of silica polymorphs is driven by the hydrolysis of the mineral surface through nucleophilic attack of water dipoles on the siloxane ($>Si-O-Si<$) bonds of the SiO_2 network. Water molecules orient their electronegative oxygen towards the Si atom, leading to a transfer of electron density to the siloxane bonds, thereby increasing their length and eventually breaking them. A series of such reactions leads to the release of hydrated Si atoms in the form of silicic acid, H_4SiO_4 [72].

The general phenomenological rate expression for surface-controlled dissolution of silica is [40]:

$$R = \frac{1}{[bSiO_2]} \frac{d[H_4SiO_4]}{dt} = k_o \cdot g \cdot A_s \cdot f(\Omega) \quad (1)$$

where $[bSiO_2]$ is the mass of $bSiO_2$ per unit volume solution, k_o is the rate coefficient, expressed in units of mass Si per unit surface area $bSiO_2$ per unit time, and is a measure of the intrinsic reactivity of the mineral surface depending primarily on the nature of the solid and temperature. The reactive surface area A_s is expressed in units of surface area per mass of solid, and is equal to the specific surface area S of the solid, in units of surface area per mass of solid, times the dimensionless term γ that represents the roughness of the surface:

$$A_s = \gamma \cdot S \quad (2)$$

The term g in Eqn. 1 is a dimensionless factor that accounts for all the solution-induced changes in the reactivity of the silica surface. In particular, g is a function of the pH and background electrolyte composition of the aqueous medium (see below).

The dissolution of silica is thermodynamically driven by the degree of undersaturation expressed as Ω in Eqn. 1. The degree of undersaturation Ω depends on the ratio between the concentration of dSi in solution (C) and the equilibrium solubility C_{eq} of the reacting solid according to:

$$\Omega = 1 - \frac{C}{C_{eq}} \quad (3)$$

The degree of undersaturation varies from a maximum value of 1 ($C = 0$) to a value of 0 for ($C = C_{eq}$), when the silica solid-aqueous solution reaches equilibrium. An important constraint on the function f in Eqn. 1 is that $f(\Omega)=0$ when $C=C_{eq}$. At $C > C_{eq}$, precipitation takes over and R represents the rate of silica precipitation.

The dissolution of biogenic silica is most commonly expressed by a linear relationship in which the dissolution rate R is linearly dependent on the degree of silica understaturation according to:

$$R = k \left(1 - \frac{C}{C_{eq}} \right) \quad (4)$$

where k is related to k_0 in Eqn. 1 according to Eqn. 5:

$$k = k_0 \cdot g \cdot A_s \quad (5)$$

The linear dissolution rate law, as expressed in Eqn. 4, has been justified on the basis of transition state theory [76, 77]. A discussion of this justification can be found elsewhere [28]. Note, however, that because mineral dissolution is a complex multi-step process there is no *a priori* reason why the linear rate law should hold.

The empirical (Arrhenius) activation energy of biogenic silica dissolution is in the order of 60 kJ mol^{-1} , which is in the same range as those reported for dissolution of synthetic amorphous silica, quartz and cristobalite [78]. These relatively high activation energies support a rate-limiting step controlled by the breaking of (strong) siloxane bonds at the solid to solution interface.

4.2 Measuring dissolution rates

In situ dissolution rates of bSiO_2 have been measured or estimated in various ways. For water column samples, Si isotopic tracer incubations provide the most direct rate determinations [79]. Alternatively, mass balance calculations using concentration distributions of silicic acid and bSiO_2 , or particulate settling fluxes during sediment trap deployments can yield estimates of net silica dissolution rates [80]. In marine sediments, dissolution rates of bSiO_2 can be estimated from the net efflux of silicic acid from the

sediments measured using benthic chambers [9, 81], or derived from pore water dSi concentration gradients at the sediment-water interface [82]. Here we mainly concentrate on laboratory techniques used for measuring dissolution kinetics of bSiO₂.

4.2.1 Batch experiments

In the laboratory, dissolution rates of bSiO₂ have been measured under controlled conditions in closed or flow-through systems. Closed system or so-called batch reactor experiments have been most commonly used mainly due to their simplicity. Typically, a sample of siliceous material is suspended in a solution which initially contains no silicic acid. The concentration of silicic acid in the solution is then monitored until the concentration of dSi no longer changes with time. The final, steady dSi concentration is then usually assumed to represent the solubility of the dissolving bSiO₂.

Fig. 3a illustrates the evolution of dSi over time in two batch dissolution experiments with cultured diatom frustules (*Thalassiosira punctigera*) and a Pliocene age marine biosiliceous ooze sample, respectively. The ooze sample was obtained from a core from the Weddell Sea, within a layer consisting nearly exclusively of fragments of frustules from the diatom species *Ethmodiscus rex*. The difference in dissolution kinetics and solubility between the two biogenic silicas, under otherwise identical experimental conditions, demonstrates the dependence on the intrinsic material and surface properties of the different samples.

If the linear dissolution rate law holds (Eqn. 4), and provided that only a negligible fraction of the initial mass of bSiO₂ dissolves during the experiment, then the data should define a straight line when plotted on a log-linear plot, with a slope equal to $-(k \cdot [bSiO_2]) / (C_{eq} \cdot V)$. The data shown in Fig. 3, however, cannot be fitted by a single rate constant k ; rather, there is an initial stage of dissolution characterized by a higher apparent rate constant. This phenomenon has been described in several previous studies [28, 46, 83-87].

It has been suggested [86, 88] that the deviation from linear kinetics at high degrees of undersaturation may represent the faster dissolution of a more reactive silica phase that is part of the frustule. A recent study presented a model demonstrating close

fits to experimental dissolution data by assuming two separate silica phases of different reactivity with surfaces that exponentially decrease during dissolution [89]. Using this model dissolution data are fitted by adjusting the ratio between the two bSiO_2 phases and the reactivity of each phase. To our knowledge, however, there is no direct evidence to suggest that the surface area of diatom frustules declines exponentially during dissolution, or that diatoms contain distinct bSiO_2 phases.

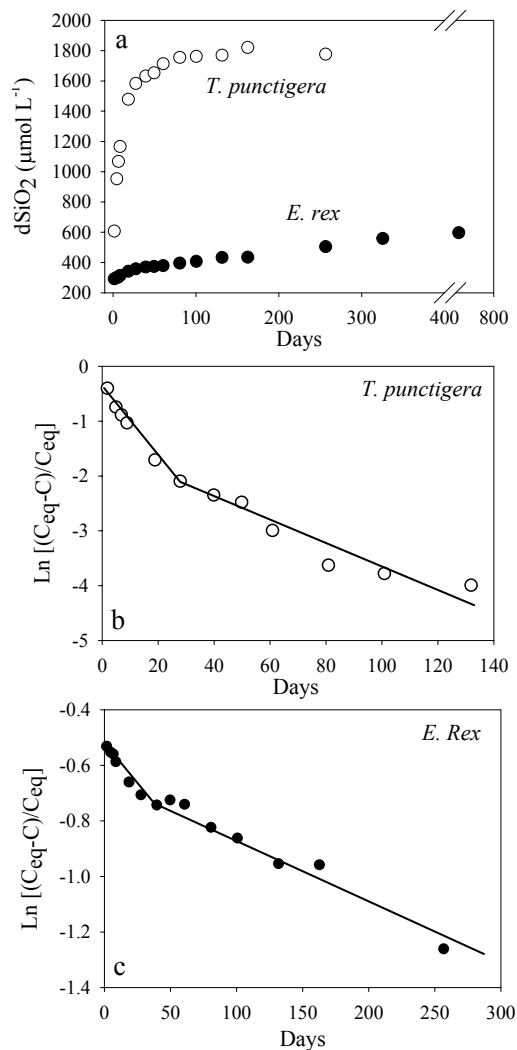


Fig. 3 Dissolution data from two batch dissolution experiments with clean (organic matter removed) diatom frustules from cultures (*T. punctigera*), and diatomaceous ooze from the S. Ocean (*E. rex*), performed in 0.1mol L^{-1} NaCl at 25°C . The initial dSi concentration was $300\mu\text{M}$. a) Build-up of dSi over time in the batch reactors. b & c) The same data plotted on log-linear plots where the slope of the line is equal to: $-(k \cdot [\text{bSiO}_2]) / (C_{\text{eq}} \cdot V)$. Note that at high undersaturation, the kinetics deviate from the simple first order rate law

In fact, the faster initial dissolution kinetics are not only observed with “fresh” diatom frustules. The dissolution curve of the 5 m.y. old diatom ooze sample from the Southern Ocean (Fig. 3c) shows a similar change in slope in the log-linear plot. Scanning Electron Microscope (SEM) images show that the *E. rex* frustules that make up the diatomite have undergone a great deal of dissolution. All frustules are fragmented and most of the finer architecture has disappeared. If a more reactive silica phase once existed in the original frustules, it is very likely that it would have dissolved away long ago.

The two-stage dissolution kinetics are also observed with synthetic amorphous silica (Fig. 4). The solid used, AEROSIL[®] OX50, is a well-characterized, single phase synthetic silica, of high physical uniformity and chemical purity. The high-resolution data from a batch dissolution experiment with AEROSIL[®] OX50 show a distinct change of slope, similar to that observed with bSiO₂ materials. These results clearly show that enhanced initial dissolution kinetics do not necessarily indicate the presence of distinct silica phases. Rather they appear to be a feature inherent to dissolution experiments. Possibly they reflect a change in dissolution mechanism as the degree of undersaturation decreases in the reactor with advancing dissolution.

4.2.2 Flow through experiments

A major drawback of batch reactor systems is that the solution composition continuously changes with time. Furthermore, the introduction of a dry sample of bSiO₂ in an aqueous solution causes an initial readjustment of the chemical structure of the solid, which may affect the build-up of the dSi in solution and complicate the interpretation of the dissolution curves. These drawbacks can be avoided by using flow-through reactors. The use of mixed flow-through reactors for measuring the dissolution kinetics of bSiO₂ was originally introduced by Van Cappellen and Qiu [77, 90] and since then applied by a number of others [29, 47, 77, 83, 90-94]. The general approach consists in suspending a mass of siliceous material in the reactor cell, which is filled with solution. An input solution of known composition is then supplied at a constant flow rate to the reactor while output solution from the reactor flows out at the same rate. Filters at the inlet and outlet prevent solid material from escaping from the reactor cell.

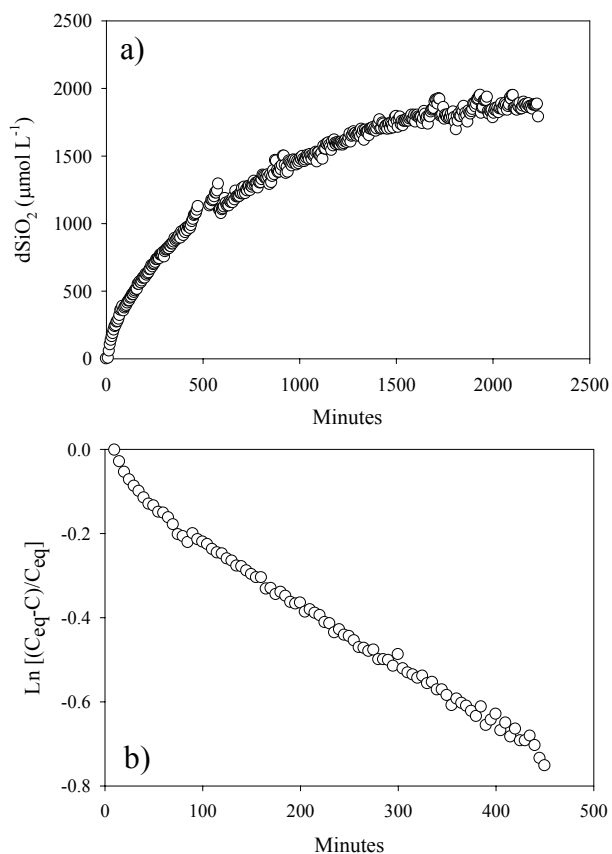


Fig. 4 High resolution batch reactor experiment with a synthetic amorphous silica (AEROSIL OX50) in 0.1 mol L⁻¹ NaCl, at 25°C, and under pH-stat (pH 8). a) Buildup of dSi inside the batch reactor monitored in real time by a nutrient auto-analyzer connected online. b) The same data on a log-linear plot demonstrating the faster initial dissolution kinetics and deviation from the linear first order dissolution rate law

If the input dSi concentration is lower than the solubility concentration of the siliceous material in the reactor then dissolution takes place, and a higher dSi concentrations is measured in the output solution. When the output dSi concentration no longer changes (i.e. steady state is reached) the dissolution rate R is calculated by:

$$R = \frac{1}{[bSiO_2]} \left(\frac{Q \cdot \Delta C}{V} \right) \quad (6)$$

where R is the steady state dissolution rate, $[bSiO_2]$ is the concentration of bSiO₂ suspended in the reactor, Q is the volumetric flow rate through the reactor, ΔC is the difference in dSi concentration between outflow and inflow solutions, and V is the

volume of the reactor cell. If both $[b\text{SiO}_2]$ and ΔC are expressed in moles of Si per liter of solution, then R is the specific dissolution rate in units of inverse time. By changing the flow rate or the composition of the input solution the system is forced into a new steady state. In this manner, multiple steady states can be achieved using the same suspension of silica in the reactor.

Results from a flow-through reactor study of the dissolution kinetics of a biosiliceous ooze sample from the Southern Ocean is shown in Fig. 5. Each point in the figure represents a steady state rate reached for a particular saturation state of the solution inside the reactor. By providing both input solutions that are undersaturated and supersaturated, both rates of dissolution and precipitation can be measured. Based on the rates, the solubility of the silica sample in the reactor can then be estimated, as it corresponds to the input dSi concentration for which there is no net dissolution or precipitation (Fig. 5). This is a great advantage of this technique, since solubility concentrations in batch reactors may take months or years to achieve.

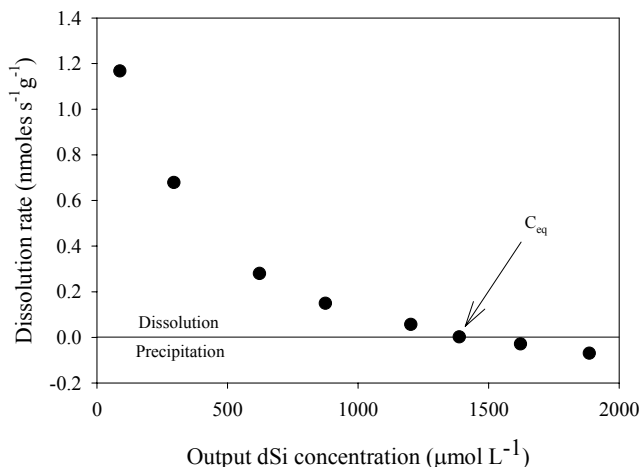


Fig. 5 Dissolution rates of a coretop biosiliceous sediment sample from the S. Ocean measured at different background dSi concentrations in a flow-through reactor experiment by Van Cappellen and Qiu, [77]. At dSi concentrations higher than the apparent solubility concentration of the sediment sample C_{eq} , dissolution ceases and precipitation takes over. Note that the dissolution rates don't appear to linearly depend on the degree of undersaturation as the simple first order rate law predicts

It can be seen in Fig. 5 that the dissolution rates do not correlate linearly with the degree of silica undersaturation, as predicted by the linear dissolution rate law. Because each point on Fig. 5 represents a dissolution rate measured at steady state, the non-linearity of the data is not due to a time-dependent change in the reactivity of bSiO₂. The non-linear dissolution kinetics may indicate a change in the reaction mechanism under variable degree of undersaturation (see previous section and [28] for an in-depth discussion).

4.3 Environmental variables

4.3.1 Temperature

Temperature strongly affects both the dissolution kinetics and solubility of bSiO₂ [46, 77, 85, 86, 90, 95]. Lawson et al. [95] determined an experimental activation energy for the dissolution of natural diatom frustules in seawater of 58 kJ mol⁻¹. Kamatani [85] reported near identical values (57-58 kJ mol⁻¹) for diatoms from cultures and natural assemblages. Dissolution rates of cultured diatom frustules (*Thalassiosira punctigera*) at 25°C, 50°C and 80°C measured in this study also yield the same activation energy of 58 kJ mol⁻¹. A number of Arrhenius activation energies reported for biogenic, synthetic and crystalline siliceous material are listed in Table 1.

Table 1 Experimental activation energies $E_{a,ex}$ for the dissolution of bSiO₂, synthetic amorphous silica, and quartz based on several experimental studies

Ref	Material	Temperature range °C	$E_{a,ex}$ kJ mol ⁻¹
[85]	Diatoms from cultures and natural assemblages	8-27	57-58
[95]	Natural diatom assemblages	7-28	58
This study	Diatom culture <i>T. punctigera</i>	25-80	58
[72]	Arkansas quartz	200-300	71.3
[96]	Synthetic silica	25-250	74
[78]	Cristobalite	150-300	70

A value for the activation energy of bSiO₂ dissolution equal to 58 kJ mol⁻¹ implies that the rate of dissolution is about 4 times slower at 4°C (average bottom ocean temperature) than it is at 21°C (average surface ocean temperature).

Because of the endothermic nature of the dissolution reaction, temperature has also a positive effect on the solubility of bSiO₂. Fig. 6 illustrates the relationship between the solubility of diatomaceous silica and temperature based on data from Lawson [95], Kamatani and Riley [46] and this study. The average linear relationship for all the data shown in Fig. 6, between 4.5°C and 28°C, is given by

$$C_{eq} = 23.8T + 936 \quad (6)$$

where T is the temperature in °C and C_{eq} is expressed in μM. This relationship predicts that a typical vertical temperature drop in the ocean from the surface (21°C) to the bottom waters (4°C) causes a drop in the solubility of bSiO₂ of over 30%.

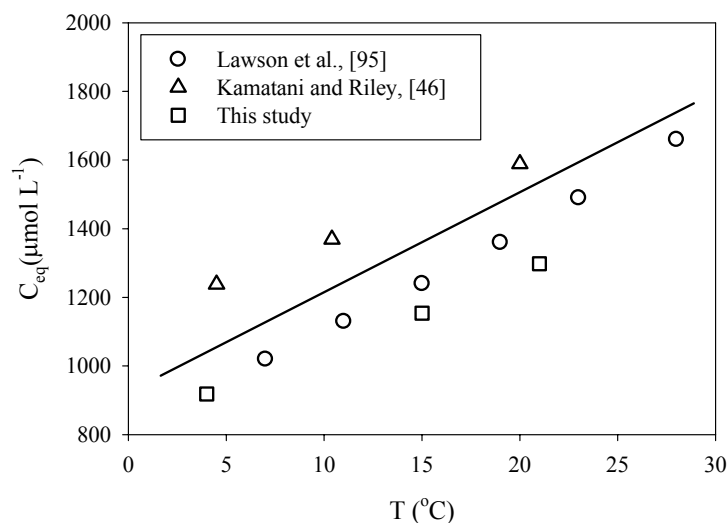


Fig. 6 Temperature dependence of the solubility concentration C_{eq} of diatomaceous silica based on solubility measurements from Lawson et al. [95], Kamatani and Riley, [46] and this study. Solubilities in this study were determined in seawater using cultured diatoms (*T. punctigera*). The linear relationship is described by Eq. 6

4.3.2 Effect of pH

Although pH is rather constant throughout the ocean, in estuarine environments, sediment pore waters, and within aggregates and fecal pellets it can vary significantly

[97-99]. As the point of zero surface charge (pH_{zpc}) of biogenic silica's ranges between 1.2-4 [100, 101], the dissolution kinetics of bSiO_2 in most natural waters should increase with increasing pH. Increasing pH leads to the deprotonation of silanol groups ($\text{>Si-OH}^0 \Leftrightarrow \text{Si-O}^- + \text{H}^+$), further facilitating the breaking of bridging siloxane bonds (>Si-O-Si<), which are believed to be the rate limiting step of the dissolution process [102].

The catalytic effect of pH on the kinetics of silica dissolution has been demonstrated for quartz [102 and references therein], vitreous silica [103], and biogenic silica [77, 94, 98, 104]. In a recent study, Loucaides et al. [94] compared dissolution rates of a number of silica samples including phytoliths, cultured diatoms, biosiliceous lake sediments and synthetic silica, for a pH typical of seawater (pH 8.1) and an average riverwater (pH 6.3). They found that on average, dissolution rates double as pH increases from 6.3 to 8.1.

Experimentally estimating the effect of pH on the dissolution kinetics of bSiO_2 can be challenging since adjusting the pH of a solution usually requires the addition of a base or acid, which consequently alters the ionic speciation and electrolyte concentration of the solution. The dissolution kinetics of silica are sensitive to changes in the ionic concentration and composition of the solution [94, 105], therefore special care must be taken in properly separating the dependence of dissolution kinetics on solution pH and electrolyte composition.

Solution pH has also been shown to affect the solubility of bSiO_2 [90, 98]. Fig. 7 illustrates the dependence of bSiO_2 solubility on pH based on experiments by Hurd [98] and Van Cappellen and Qiu [90]. The latter authors found, using flow-through experiments, that the solubility of a siliceous ooze from the Southern Ocean increases by 10% between pH 6 and 8. At higher pH the effect on solubility is stronger; although in most oceanic and lacustrine environments pH values above 8.5 are uncommon. In some shallow-water ecosystems, however, benthic photosynthetic activity can lead to elevated pH values ($\text{pH}>9$) in the sediments.

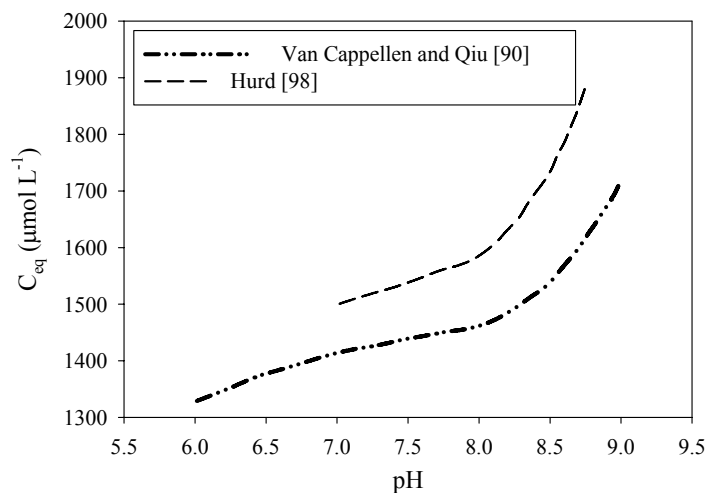


Fig. 7 Apparent solubility concentrations C_{eq} of biosiliceous sediments from the S. Ocean and Central Equatorial Pacific as a function of pH, based on the experiments of Van Cappellen and Qiu [90] and Hurd [98] respectively

4.3.3 Pressure

The effect of pressure on the dissolution kinetics and solubility of bSiO_2 is of potential interest when oceanic settings are considered. To our knowledge, no experimental work has been published on the effect of pressure on the solubility and kinetics of bSiO_2 . To this date, the pressure dependence of bSiO_2 solubility has been estimated based on experiments with synthetic amorphous silica [106].

Willey [106] studied the solubility of amorphous silica at pressures up to 1240 bar. Her experiments showed that the solubility of synthetic silica increases with pressure. Below ~ 270 bar the solubility increases by $\sim 0.70 \mu\text{M bar}^{-1}$ and between ~ 270 and 1240 bar by $\sim 0.35 \mu\text{M bar}^{-1}$. Willey's [107] data suggest that the solubility at 400 bar (equivalent to an average oceanic water depth of 4000 m) is about 17% higher than at 1 bar. Recently, Loucaides et al. (In preparation) studied the solubility of diatom frustules, at pressures between 1 and 700 bar, in laboratory and field experiments. In contrast with the work of Willey [106] their results showed that the solubility of diatom frustules decreases when pressure increases from 1 to ~ 200 bar. Around 200 bar, however, their data imply a reversal in the pressure dependence and a gradual increase in solubility with pressure to 700 bar. According to their results, the solubility of diatom

frustule at 400 bar is about 15% higher than at atmospheric pressure. This estimate is within experimental error of that by Willey [106].

The available data indicates that the effect of pressure on the solubility of bSiO₂ cannot not be ignored. Considering an average oceanic water depth of 4000 m, however, a typical drop in temperature of about 20°C can have a far more significant effect on solubility than an equivalent 400 bar increase in pressure. Nevertheless the anomalous dependence of bSiO₂ solubility on pressure suggests that further experimental work is necessary in order to understand the effect of pressure on the recycling efficiency of bSiO₂.

4.3.4 *Electrolyte composition*

It has been well documented that dissolution rates of quartz are significantly enhanced by the presence of alkali salts [72, 102, 105, 107-109]. The exact mechanism by which the presence of these salts enhances the dissolution process is not yet fully understood. Dove [107] proposed that the presence of alkali cations enhances the nucleophilic properties of water, thus increasing the frequency of hydrolysis attacks at the silica surface. Recently, Loucaides et al. [94] found that the dissolution rates of a number of bSiO₂ samples were on average 5 times higher in seawater than in freshwater (Fig. 8). They also observed an increase in dissolution rates in freshwater that was augmented with alkali salts (NaCl, KCl, MgCl₂ and CaCl₂), thus confirming the catalyzing effect of alkali and earth alkali cations on silica dissolution.

The catalytic effect of salts on the dissolution of bSiO₂ may explain the generally more efficient recycling of bSiO₂ in marine environments, compared to continental aquatic environments. Furthermore it points to the need to reevaluate the role of estuaries and coastal embayments in the global bSiO₂ cycle. In these environments, favorable conditions lead to high biosiliceous productivity that contributes to a significant fraction of the world's bSiO₂ production [110, 111], while at the same time they serve as filters for bSiO₂ produced on land [53, 112, 113]. Salinity enhanced dissolution along the land to ocean transition zone may be an important source of nutrient Si to the global coastal ocean that has to date been underestimated.

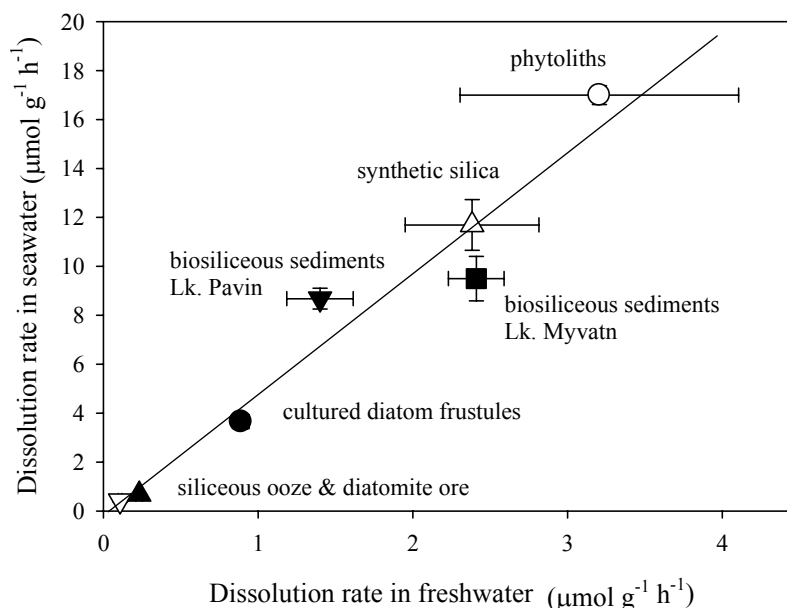


Fig. 8 Dissolution rates in seawater versus dissolution rates in freshwater at 25°C of several siliceous materials. The strong linear relationship ($r^2=0.95$) indicates on average 5 times higher dissolution rates in seawater. (Figure adapted from Loucaides et al. [94])

5 Below the sediment-water interface

Biogenic silica that survives dissolution in the water column is deposited at the seafloor and slowly becomes buried. Dissolution continues in the sediments leading to an efflux of dSi to the bottom waters. Typically pore water silicic acid concentrations increase downward until they level off at a quasi-constant value at depths of around 5-30 cm below the sediment-water interface [9, 80, 90, 91, 98, 114-116]. This quasi-constant or asymptotic dSi concentration has often been interpreted as the equilibrium concentration of the biogenic silica buried in the sediments. This interpretation, however, poses the following problems: a) there is considerable spatial variation in the asymptotic dSi concentration between various sediments, b) the asymptotic dSi concentrations found in the sediments are well below solubility values measured directly on bSiO₂ [29, 43, 84, 86, 94, 95], and c) solubility values of bSiO₂ collected in sediment traps can be considerably higher than asymptotic dSi values measured in the underlying sediments

[91]. Similarly, when pore water dSi profiles are fitted to early diagenetic models, the resulting dissolution rate constants are highly variable and orders of magnitude lower than dissolution rate constants measured on cleaned biogenic opal [117, 118].

5.1 Opal-detrital interactions

Early diagenetic reactions involving bSiO₂ and lithogenic constituents in sediments have been invoked to explain the observed variations in asymptotic pore water dSi concentrations and benthic dSi fluxes in the deep and coastal ocean [9, 82, 119-122]. Dixit et al. [29] found that the build-up of dSi, in batch experiments where bSiO₂ and either kaolinite or ground basalt were suspended together in 0.7 M NaCl solution, decreased systematically as the mass ratio of the lithogenic constituent to bSiO₂ increased. This inverse relationship is reminiscent of that observed between the asymptotic pore water dSi concentration and the abundance of lithogenic mineral compounds, relative to that of bSiO₂, in deep-sea sediments of the Southern Ocean [77], the Equatorial Pacific and the North Atlantic [91], as well as the Atlantic sector of the Southern Ocean [119].

Van Cappellen and Qiu [90] suggested that asymptotic dSi concentrations obtained from heterogeneous samples in flow-through or batch experiments, should be treated as “apparent” saturation levels and not as the actual solubility of the biogenic fraction. Similarly in marine sediments, asymptotic porewater dSi concentrations represent weighted averages of the solubilities of the various silicate phases present.

5.2 Aluminum-bSiO₂ interactions

Previous studies dealing with variations of pore water dSi concentrations and bSiO₂ preservation in marine sediments have stressed the role of Al uptake by biosiliceous debris [29, 43, 77, 123]. Diatom frustules retrieved from Congo Fan sediments have clearly shown that bSiO₂ can take up significant amounts of Al during early diagenesis [123]. Results from experimental studies further demonstrate that sorption of aluminum reduces both the solubility and dissolution kinetics of bSiO₂ [43, 74, 123]. Fig. 9 presents results from two studies [28, 43] where bulk solubilities of

diatom frustules (cultured diatoms, open ocean diatoms, core sediments) were measured in batch reactors. Both studies demonstrate the negative effect of Al sorption on the solubility of bSiO₂.

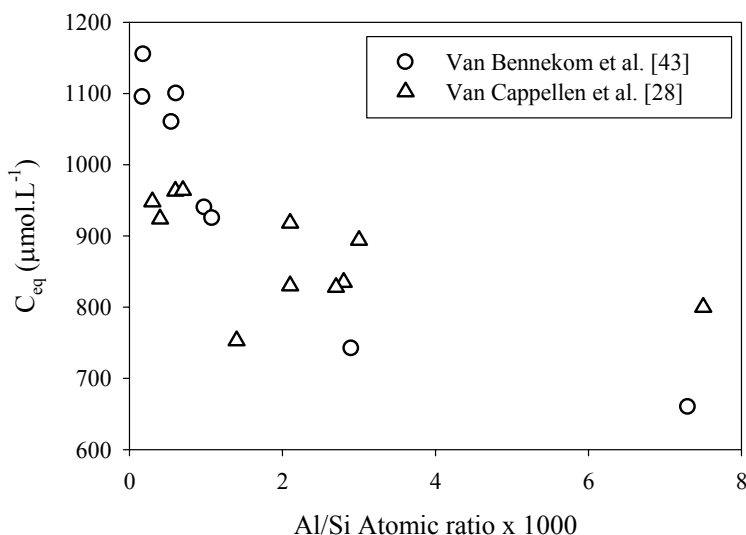


Fig. 9 Relationship between bSiO₂ solubility C_{eq} and its aluminum content expressed here as the Al/Si atomic ratio. Data from Van Bennekom et al. [43] and Van Cappellen et al., [40]

In the water column, because of the low levels of dissolved Al, Al to Si atomic ratios of natural plankton assemblages don't exceed 10⁻⁴, while higher ratios are generally found in diatoms buried in the sediments [28, 29, 43]. Therefore, Al sorption mostly takes place in the sediments where Al concentrations are higher due to the dissolution of terrigenous aluminosilicate minerals. The net result is that Al uptake results in a slower rate and extent of silica dissolution, thereby increasing the preservation of reactive Si in the sediments.

Gehlen et al. [124] presented direct evidence of structural association of Al with diatoms from cultures and pelagic assemblages. Based on the results of a number of spectroscopic techniques (XAS, XANES, EXAFS) the authors found that Al was present within the silica framework in tetrahedral coordination. The authors proposed that Al was probably incorporated within the frustules during biomineralization. In a later study, Koning et al. [125] cultured diatoms in Al-enriched seawater, and for comparison incubated clean (organic matter removed) diatom frustules in Al-rich seawater for several

weeks. The authors found that the Al in seawater did not affect the Al content of the live diatoms. In contrast, the Al/Si atomic ratio of the clean diatom frustules incubated in the Al-rich seawater significantly increased with time. These results suggest that Al sorption takes place after diatoms die (secondary uptake) rather than during biosynthesis. In line with the results of Gehlen et al. [124], the authors found that Al was present in the incubated frustules mostly in tetrahedral coordination. Furthermore, results from N₂ BET analyses suggest that the incubation of the frustules in Al-rich seawater results to significant changes in the frustules surface area and porosity. Based on these results, the authors proposed, that Al was incorporated, not in the frustule itself, but in an aluminosilicate layer formed on the surface of the frustules. As proposed by Van Cappellen and Qiu [77], Al uptake by bSiO₂ exhibits a continuum from adsorption of Al³⁺ ions to surface sites to incorporation into newly formed phases associated with the frustules.

5.3 Reverse weathering in continental margin sediments

The main sink for reactive Si in the oceans is burial in marine sediments, about half of which occurs in nearshore and continental shelf sediments [113, 126]. These sediments are also the main recipients of particulate matter originating from the continents, especially terrigenous clays. It has long been suspected that early diagenetic interactions in continental margin sediments exert a major control on the biogeochemical cycle of Si and, ultimately, on the siliceous productivity of the oceans [127].

Michalopoulos et al. [128] discovered diatom frustules in deltaic sediments of the Amazon River that were partly or fully converted into authigenic K-rich and Fe-rich aluminosilicate material. The authors demonstrated through laboratory incubations that the conversion of diatom frustules into clays can be completed in less than 23 months. Loucaides et al. [129] incubated cultured diatom frustules in suspensions of terrigenous sediments from the Mississippi River Delta and the Congo River Fan. The incubations were carried out in the laboratory and deployed along mooring lines at sea for 1 to 2 years. Chemical and microscopic analyses of the incubated frustules at the end of the experiments revealed the transfer of chemical elements from seawater (e.g., Mg, K) and

from the clay-rich sediments (e.g., Al, Fe, Mn) to the frustules. The latter resulted in the formation of a variety of new mineral precipitates, including aluminosilicate and magnesian silicate phases, deposited on the surfaces of the frustules. In experiments performed under oxic conditions, phosphate-rich ferric iron oxyhydroxides also formed.

Interactions between biogenic silica, seawater and lithogenic minerals enhance the removal of reactive silicon from the ocean system through sedimentary burial. Previous estimates of burial of reactive Si in river deltas may have been biased by the commonly used leaching techniques for bSiO₂, which fail to measure the diagenetically altered material. Recent estimates based on improved leaching techniques suggest that river deltas may be a far more important marine sink of reactive Si than previously thought [121, 122]. In addition, uptake by biogenic silica and the precipitation of secondary mineral products may affect the biogeochemical cycles of other key biological (e.g., Fe, P) and geochemical (e.g., Mg, Al) elements. While some of these processes have long been recognized, they are rarely considered in budgets and model studies of biogeochemical cycles.

6. Surface reactivity and “aging” of bSiO₂

The dissolution rate of bSiO₂ dissolution is directly related to the surface area of the solid-solution interface. Differences among species and environmental conditions during growth are responsible for large inter and intra-species variations in specific surface areas (see section 3.1). Hurd and Theyer [130] found that BET specific surface area values of bSiO₂ extracted from sediments of the Central Equatorial Pacific, declined from about 250 m²·g⁻¹ to less than 50 m²·g⁻¹ in a period of 40 million years (~2100 cm below sediment/water interface). Since net dissolution of bSiO₂ in deep sea sediments is limited to the topmost few centimeters [93, 130] according to the results of Hurd and Treyer [130] the specific surface area does not significantly change enough to affect solubility or dissolution kinetics.

Van Cappellen [93] however, observed that even though the BET surface area of bulk bSiO₂-rich Southern Ocean sediments was practically constant down to 30 cm depth, the reactivity of the bSiO₂ steadily declined. Since elemental and microscopic

analyses showed no changes in mineral composition or any diagenetic alterations throughout the sediment cores, the author proposed that the gradual loss of reactivity with depth was due to the reduction of the specific reactive surface area of bSiO₂ (not to be confused with the BET specific surface area). He further proposed that the reactivity of bSiO₂ decreases with depth in the sediments due to a progressive loss of reactive sites, which he defined as “aging”. Later experiments on the same sediment samples demonstrated that the decrease in adsorption capacity for exchangeable Co⁺² ions (which correlates with the number of adsorption sites on the silica surfaces) with depth, correlated positively with that of the measured dissolution rates [77].

Reactive site densities of bSiO₂ have also been measured using acid-base titrations [30, 100, 101]. Dixit and Van Cappellen [100] found that reactive site densities were systematically lower for biosiliceous material found in marine sediments than cultured or planktonic diatoms. Loucaides et al. [30] observed similar a pattern when comparing the surface charge density of freshly cultured diatoms and plant phytoliths with that of lacustrine and marine biosiliceous sediments.

The progressive alteration (aging) of bSiO₂ in the water column and oceanic sediments has also been proposed based on spectroscopic evidence [47, 92]. Schmidt et al. [92] used FTIR spectroscopic analyses to estimate the ratio between siloxane (>Si-O-Si<) and silanol (>Si-OH) groups. FTIR spectra of silica show peaks at both 800cm⁻¹ and 950cm⁻¹ corresponding to silanol and siloxane bonds respectively. The ratio between the integrated intensities of the 800 and 1100 cm⁻¹ ($A_{800\text{ cm}^{-1}}/A_{1100\text{ cm}^{-1}}$) absorption bands can be used as an indication of the degree of organization or ordering of the SiO₂ framework [131]. The authors performed the analysis on a variety of biosiliceous samples including natural phytoplankton, cultured diatoms, sediment trap material, surface sediments, and biosiliceous material from deeper sediments. As illustrated in Fig. 10, their analyses showed that the intensity ratio between siloxane and silanol peaks increased systematically with the age of the sample (i.e. fresh diatoms< sediment trap diatoms<surface sediments<deep sediments) suggesting that aging starts as soon as the silica is exposed to seawater after death of the organism. In a related study, Rickert et al [47] demonstrated that the decrease of reactive silanol density observed by Schmidt et al.

[92] corresponded to a reduction of dissolution rates by more than two orders of magnitude.

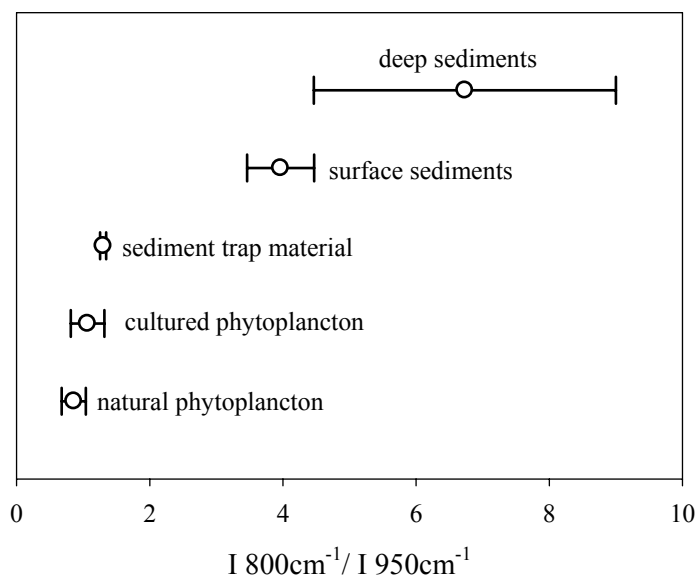


Fig. 10 Ratio between peak intensities at 800cm^{-1} and 950cm^{-1} that correspond to ($>\text{Si-O-Si}<$) and ($<\text{Si-O}$) groups respectively as measured by FTIR spectroscopy [92]

7. Summary and Perspectives

The dissolution of bSiO_2 sustains a significant fraction of the oceanic primary productivity by controlling the availability of nutrient Si in the ocean. Diatoms, limited by the availability of dSi , are an important link between the marine Si and C cycles.

The apparent spatial and temporal variability in the dissolution efficiency of bSiO_2 is most likely responsible for the so called “opal paradox”. This work suggests that this variability, is controlled by a number of geochemical and ecosystem processes both during biosynthesis and after diatoms die.

Environmental conditions during biomineralization (i.e. temperature, light, nutrient availability, grazing) significantly affect the silicification of diatoms by controlling their growth rates. Frustule silicification is enhanced when growth rates are low but also when dSi concentrations are high. On the contrary, fast growth rates during

diatom blooms generally lead to the production of less silicified frustules. While dSi limitation doesn't significantly affect growth rates, it has a negative effect on the silicification of diatom frustules.

Because of their higher resistance to weathering, highly silicified diatoms are regarded as more efficient exporters of Si but also C to the deep. During diatom blooms, enhanced utilization of CO₂ through high primary productivity may not inherently correspond to higher carbon export. Instead, CO₂ uptake under these conditions may only be temporary, since lightly silicified diatoms are physically incapable of transferring the carbon below the photic zone. On the contrary, during fast diatom growth, carbon export to the deep ocean may be exclusively controlled by grazers who prefer smaller and more lightly silicified diatoms and through the formation of fecal pellets can efficiently transfer C and Si to the deep ocean.

Immediately after death, the fate of diatom frustules depends on the efficiency in which bacteria can consume the protective organic coatings. In the open ocean, bacteria have ample time to break down the organic layer while diatoms are sinking. In shallow waters, however, it's possible that some diatoms can reach the sediments with the organic layer intact. Since the dissolution of diatom frustules is limited by the presence of the organic layer, in such shallow environments the efficiency in which bacteria can consume the organic layer can be critical.

Sinking velocities of diatom frustules are enhanced when single cells aggregate together into larger and less buoyant particles. Aggregation is enhanced by the presence of TEP which its production and adhesivity can be a function of several parameters including grazing pressure, nutrient availability, light intensity, and bacterial activity. During diatom blooms, C and Si export can be significantly enhanced by aggregation, which along with grazing (and the formation of fecal pellets) can be the main processes responsible for the Si and C flux to the deep ocean.

Once free from organic matter, the dissolution efficiency of diatom frustules is mainly controlled by the physicochemical properties of both the mineral's surface as well as the aqueous medium. The dissolution rates of sinking diatom frustules are strongly controlled by the changing temperature and pressure throughout the water column.

Similarly along the land to ocean transition, dissolution rates change significantly as a function of salinity and pH.

In the sediments, recycling of bSiO₂ continues although interactions with pore water constituents (mainly Al), build-up of dSi, and aging processes reduce the rate of dissolution. Interactions between bSiO₂ and elements released from the sediments play an important role in the global Si cycle by providing diagenetic pathways of silica preservation that can be far more rapid than the classic opal-A>opal-CT>quartz recrystallization generally considered. Relatively recent evidence suggest that diatoms deposited in clay-rich sediments can be completely transformed to authigenic clays in less than 3 years, while in other cases diatom frustules provide the substrate for the formation of aluminosilicate coatings that can protect the frustules from dissolution. It has been proposed that the interaction between bSiO₂ and Al can lead to alternative diagenetic pathways, with smectites or zeolites as intermediates.

Better knowledge of the possible interaction between bSiO₂ and other elements is vital in order to better characterize links between different elemental cycles but also identify elemental sinks that to date have been overlooked. A substantial amount of research has been conducted, studying the interactions of Al and Si in the sediments but also in the water column during biomineralization. To our knowledge, however, little work has been done on the effect of other elements on the preservation of bSiO₂, even though evidence suggests that such interactions could exist.

Recent spectroscopic evidence suggest that aging mechanisms can reduce the reactivity of bSiO₂ even during sinking. These mechanisms still remain unknown but recent advances in spectroscopic and analytical techniques may be able to detect minor changes in the chemical structure and surface chemistry of amorphous silica. Laboratory aging experiments with cultured diatom frustules combined with spectroscopic techniques have the potential to elucidate these early diagenetic transformations of bSiO₂.

This paper presents the great complexity involved in the recycling of bSiO₂ in the ocean. Biomineralization, dissolution, and preservation processes are dependent on a variety of physical, chemical, and biological factors that together define the relationship between bSiO₂ production and preservation. Environmental parameters including, temperature and nutrient availability can affect the fate of bSiO₂ in many levels from

biomineralization to burial. Aware of this complexity we have to realize that simple interpretations of the sedimentary record based on diatom taphonomy can be a risky and misleading while instead, a better understanding of each forcing factor must be carefully evaluated. Most importantly, due to the fact that the recycling efficiency of bSiO_2 is closely coupled to the cycle of C, good knowledge of the dynamics involved is vital to better understand the significance and functioning of the biological pump.

8. References

1. DeMaster, D.J., *The supply and accumulation of silica in the marine environment*. *Geochimica et Cosmochimica Acta*, 1981. 45(10): p. 1715-1732.
2. Ragueneau, O., et al., *A review of the Si cycle in the modern ocean: recent progress and missing gaps in the application of biogenic opal as a paleoproductivity proxy*. *Global and Planetary Change*, 2000. 26(4): p. 317-365.
3. Tréguer, P., et al., *The silica balance in the world ocean - a reestimate*. *Science*, 1995. 268(5209): p. 375-379.
4. Nelson, D.M., et al., *Production and Dissolution of Biogenic Silica in the Ocean - Revised Global Estimates, Comparison with Regional Data and Relationship to Biogenic Sedimentation*. *Global Biogeochemical Cycles*, 1995. 9(3): p. 359-372.
5. Ragueneau, O., et al. (2006) *Si and C interactions in the world ocean: Importance of ecological processes and implications for the role of diatoms in the biological pump*. *Global Biogeochemical Cycles* 20, DOI: 10.1029/2006GB002688.
6. Conley, D.J. (2002) *Terrestrial ecosystems and the global biogeochemical silica cycle*. *Global Biogeochemical Cycles* 16, DOI: 10.1029/2002GB001894.
7. Pondaven, P., et al., *Resolving the 'opal paradox' in the Southern Ocean*. *Nature*, 2000. 405(6783): p. 168-172.
8. Koning, E., et al., *Selective preservation of upwelling-indicating diatoms in sediments off Somalia, NW Indian Ocean*. *Deep Sea Research Part I: Oceanographic Research Papers*, 2001. 48(11): p. 2473-2495.
9. McManus, J., et al., *Early diagenesis of biogenic opal: Dissolution rates, kinetics, and paleoceanographic implications*. *Deep Sea Research Part II: Topical Studies in Oceanography*, 1995. 42(2-3): p. 871-903.

10. Ryves, D.B., et al., *Experimental diatom dissolution and the quantification of microfossil preservation in sediments*. Paleogeography, Paleoclimatology, Peleocology, 2001. 172: p. 99-113.
11. Barker, P., *Differential diatom dissolution in Late Quaternary sediments from Lake Manyara, Tanzania: an experimental approach*. Journal of Paleolimnology, 1992. 7(3): p. 235-251.
12. Lotter, A.F., et al., *Modern diatom, cladocera, chironomid, and chrysophyte cyst assemblages as quantitative indicators for the reconstruction of past environmental conditions in the Alps .I. Climate*. Journal of Paleolimnology, 1997. 18(4): p. 395-420.
13. Abelmann, A., R. Gersonde, and V. Spiess, *Pliocene - Pleistocene paleoceanography in the Weddell Sea - Siliceous microfossil evidence*, in *Geological history of the polar oceans: Arctic versus Antarctic*, U. Bleil and J. Thiede, Editors. 1988, Kluwer Academic Publishers: Bremen. p. 729-759.
14. Rocha, C.L.D.L., *Opal-based isotopic proxies of paleoenvironmental conditions*. Global Biogeochemical Cycles, 2006. 20(GB4S09).
15. Martin-Jezequel, V., H. M., and M.A. Brzezinski, *Silicon metabolism in diatoms: implications for growth*. Journal of Phycology, 2000. 36: p. 821-840.
16. Brzezinski, M.A., R.A. Olson, and S.W. Chisholm, *Silicon availability and cell-cycle progression in marine diatoms*. Marine Ecology Progress Series, 1990. 67: p. 83-96.
17. Nelson, D.M. and Q. Dortch, *Silicic acid depletion and silicon limitation in the plume of the Mississippi River: evidence from kinetic studies in spring and summer*. Marine Ecology Progress Series, 1996. 136: p. 163-178.
18. Paasche, E., *Silicon and the ecology of marine plankton diatoms. I. Thalassiosira pseudonana (Cyclotella nana) grown in a chemostat with silicate as limiting nutrient*. Marine Biology, 1973. 19(2): p. 117-126.
19. Claquin, P., et al., *Uncoupling of silicon compared with carbon and nitrogen metabolisms and the role of the cell cycle in continuous cultures of thalassiosira pseudonana (Bacillariophyceae) under light, nitrogen, and phosphorous control*. Journal of Phycology, 2002. 38(5): p. 922-930.
20. Davis, C.O., *Continuous culture of marine diatoms under silicate limitation. II. Effect of light intensity on growth and nutrient uptake of Skeletonema constantum*. Journal of Phycology, 1976. 12(3): p. 291-300.
21. Taylor, N.J., *Silica incorporation in the diatom Coscinodiscus granii as affected by light intensity*. British Phycological Journal, 1985. 20: p. 365-374.

22. Durbin, E.G., *Studies in the autoecology of the marine diatom Thalassiosira nordenskioeldii. II. The influence of cell size on growth rate and carbon, nitrogen, chlorophyll a and silica content.* Journal of Phycology, 1977. 13: p. 150-155.
23. Paasche, E., *Silicon Content of Five Marine Plankton Diatom Species Measured with a Rapid Filter Method.* Limnology and Oceanography, 1980. 25(3): p. 474-480.
24. Harrison, P.J., H.L. Conway, and R.C. Dugdale, *Marine diatoms grown in chemostats under silicate or ammonium limitation. I. Cellular chemical composition and steady-state growth kinetics of Skeletonema costatum.* Marine Biology, 1976. 35(2): p. 177-186.
25. Harrison, P.J., et al., *Marine diatoms grown in chemostats under silicate or ammonium limitation. III. Cellular chemical composition and morphology of Chaetoceros debilis, Skeletonema costatum, and Thalassiosira gravida.* Marine Biology, 1977. 43(1): p. 19-31.
26. Conley, D.J. and S.S. Kilham, *Differences in silica content between marine and freshwater diatoms.* Limnology and Oceanography, 1989. 34(1): p. 205-213.
27. Pondaven, P., et al., *Grazing-induced Changes in Cell Wall Silicification in a Marine Diatom.* Protist, 2007. 158(1): p. 21-28.
28. Van Cappellen, P., S. Dixit, and J.E.E. Van Beusekom (2002) *Biogenic silica dissolution in the oceans: Reconciling experimental and field-based dissolution rates.* Global Biogeochemical Cycles 16, DOI: 10.1029/2001GB001431.
29. Dixit, S., P. Van Cappellen, and A.J. van Bennekom, *Processes controlling solubility of biogenic silica and pore water build-up of silicic acid in marine sediments.* Marine Chemistry, 2001. 73(3-4): p. 333-352.
30. Loucaides, S., T. Behrends, and P. Van Cappellen, *Reactivity of biogenic silica: Surface versus bulk charge density.* Geochimica et Cosmochimica Acta, 2010. 74(2): p. 517-530.
31. Brzezinski, M.A., *The Si:C:N ratio of marine diatoms: interspecific variability and the effect of some environmental variables.* Journal of Phycology, 1985. 21(3): p. 347-357.
32. Vrieling, E.G., et al., *Nanoscale uniformity of pore architecture in diatomaceous silica: A combined small and wide angle X-ray scattering study.* Journal of Phycology, 2000. 36(1): p. 146-159.
33. Kemp, A.E.S., et al., *Production of giant marine diatoms and their export at oceanic frontal zones: Implications for Si and C flux from stratified oceans.* Global Biogeochemical Cycles, 2006. 20(GB4S04).

34. Kemp, A.E.S., et al., *The "Fall dump" -- a new perspective on the role of a "shade flora" in the annual cycle of diatom production and export flux*. Deep Sea Research Part II: Topical Studies in Oceanography, 2000. 47(9-11): p. 2129-2154.
35. Smetacek, V., *Oceanography: The giant diatom dump*. Nature, 2000. 406(6796): p. 574-575.
36. Mackenzie, F.T., M. Stoffyn, and R. Wollast, *Aluminum in Seawater: Control by Biological Activity*. Science, 1978. 199(4329): p. 680-682.
37. Menzel, D.W., E.M. Hulburt, and J.H. Tyther, *The effects of enriching Sargasso sea water on the production and species composition of the phytoplankton*. Deep Sea Research and Oceanographic Abstracts, 1963. 10(3): p. 209-219.
38. Stoffyn, M., *Biological Control of Dissolved Aluminum in Seawater: Experimental Evidence*. Science, 1979. 203(4381): p. 651-653.
39. Gensemer, R.W., *Role of aluminum and growth rate on changes in cell size and silica content of silica-limited populations of Asterionella ralfsii var. Americana (Bacillariophyceae)* Journal of Phycology, 1990. 26(2): p. 250-258.
40. Van Cappellen, P., S. Dixit, and M. Gallinari, *Biogenic silica dissolution and the marine Si cycle: kinetics, surface chemistry and preservation*. Océanis, 2002. 28(3-4): p. 417-454.
41. Van Beusekom, J.E.E., *Wechselwirkungen zwischen gelösten Aluminium und Phytoplankton in marinen Gewässern*. 1989, Hamburg University. p. 164.
42. Vrieling, E.G., W.W.C. Gieskes, and T.P.M. Beelen, *Silicon deposition in diatoms: Control by the pH inside the silicon deposition vesicle*. Journal of Phycology, 1999. 35(3): p. 548-559.
43. Van Bennekom, A.J., B.A.G. L, and N.R. F, *Dissolved aluminium in the Weddell-Scotia Confluence and effect of Al on the dissolution kinetics of biogenic silica*. Marine Chemistry, 1991. 35: p. 423-434.
44. Hecky, R.E., et al., *The amino acid and sugar composition of diatom cell-walls*. Marine Biology, 1973. 19(4): p. 323-331.
45. Bidle, K.D. and F. Azam, *Bacterial Control of Silicon Regeneration from Diatom Detritus: Significance of Bacterial Ectohydrolases and Species Identity* Limnology and Oceanography 2001. 46(7): p. 1606-1623.
46. Kamatani, A. and J.P. Riley, *Rate of dissolution of diatom silica walls in seawater*. Marine Biology, 1979. 55(1): p. 29-35.

47. Rickert, D., M. Schluter, and K. Wallmann, *Dissolution kinetics of biogenic silica from the water column to the sediments*. *Geochimica et Cosmochimica Acta*, 2002. 66(3): p. 439-455.
48. Patrick, S. and A.J. Holding, *The effect of bacteria on the solubilization of silica in diatom frustules*. *Journal of applied bacteriology*, 1985. 59(1): p. 7-16.
49. Bidle, K.D. and F. Azam, *Accelerated dissolution of diatom silica by marine bacterial assemblages*. *Nature*, 1999. 397(6719): p. 508-512.
50. Ward, D.M., et al., *A Natural View of Microbial Biodiversity within Hot Spring Cyanobacterial Mat Communities*. *Microbiology and Molecular Biology Reviews*, 1998. 62(4): p. 1353-1370.
51. Tamburini, C., et al., *Pressure effects on surface Mediterranean prokaryotes and biogenic silica dissolution during a diatom sinking experiment*. *Aquatic Microbial Ecology*, 2006. 43(3): p. 267-276.
52. Broughton, L.C. and K.L. Gross, *Patterns of diversity in plant and soil microbial communities along a productivity gradient in a Michigan old-field*. *Oecologia*, 2000. 125(3): p. 420-427.
53. Roubeix, V., S. Becquevort, and C. Lancelot, *Influence of bacteria and salinity on diatom biogenic silica dissolution in estuarine systems*. *Biogeochemistry*, 2008. 88(1): p. 47-62.
54. Corzo, A., J.A. Morillo, and S. Rodríguez, *Production of transparent exopolymer particles (TEP) in cultures of Chaetoceros calcitrans under nitrogen limitation*. *Aquatic Microbial Ecology*, 2000. 23: p. 63-72.
55. Drapeau, D.T., H.G. Dam, and G. Grenier, *An Improved Flocculator Design for Use in Particle Aggregation Experiments*. *Limnology and Oceanography*, 1994. 39(3): p. 723-729.
56. Passow, U., *Transparent exopolymer particles (TEP) in aquatic environments*. *Progress In Oceanography*, 2002. 55(3-4): p. 287-333.
57. Passow, U., A. Engel, and H. Ploug, *The role of aggregation for the dissolution of diatom frustules*. *FEMS Microbiology Ecology*, 2003. 46(3): p. 247-255.
58. Malej, A. and R.P. Harris, *Inhibition of copepod grazing by diatom exudates: a factor in the development of mucus aggregates*. *Marine Ecology Progress Series*, 1993. 96: p. 33-42.
59. Staats, N., et al., *Oxygenic photosynthesis as driving process in exopolysaccharide production of benthic diatoms*. *Marine Ecology Progress Series*, 2000. 193: p. 261-269.

60. Passow, U., et al., *The origin of transparent exopolymer particles (TEP) and their role in the sedimentation of particulate matter*. Continental Shelf Research, 2001. 21(4): p. 327-346.
61. Alldredge, A.L. and C. Gotschalk, *In Situ Settling Behavior of Marine Snow*. Limnology and Oceanography, 1988. 33(3): p. 339-351.
62. Alldredge, A.L. and M.W. Silver, *Characteristics, dynamics and significance of marine snow*. Progress In Oceanography, 1988. 20(1): p. 41-82.
63. Moriceau, B., et al., *Evidence for reduced biogenic silica dissolution rates in diatom aggregates*. Marine Ecology Progress Series, 2007. 333: p. 129-142.
64. Alldredge, A.L. and Y. Cohen, *Can Microscale Chemical Patches Persist in the Sea? Microelectrode Study of Marine Snow, Fecal Pellets*. Science, 1987. 235(4789): p. 689-691.
65. Alldredge, A.L., et al., *The Physical Strength of Marine Snow and its Implications for Particle Disaggregation in the Ocean*. Limnology and Oceanography, 1990. 35(7): p. 1415-1428.
66. Simon, M., et al., *Microbial ecology of organic aggregates in aquatic ecosystems*. Aquatic Microbial Ecology, 2002. 28: p. 175-211.
67. Hamm, C.E., et al., *Architecture and material properties of diatom shells provide effective mechanical protection*. Nature, 2003. 421(6925): p. 841-843.
68. Turner, J.T., et al., *Zooplankton feeding ecology: does a diet of Phaeocystis support good copepod grazing, survival, egg production and egg hatching success?* Journal of Plankton Research, 2002. 24(11): p. 1185-1195.
69. Fowler, S.W. and N.S. Fisher, *Viability of marine phytoplankton in zooplankton fecal pellets*. Deep Sea Research Part A. Oceanographic Research Papers, 1983. 30(9): p. 963-969.
70. Platt, T., et al., *Photosynthetically-Competent Phytoplankton from the Aphotic Zone of the Deep Ocean*. Marine Ecology Progress Series, 1983. 10: p. 105-110.
71. Schultes, S., *The role of mesozooplankton grazing in the biogeochemical cycle of silicon in the Southern Ocean*, in *Biology and Chemistry*. 2004, University of Bremen: Bremen. p. 172.
72. Dove, P.M. and D.A. Crerar, *Kinetics of quartz dissolution in electrolyte solutions using a hydrothermal mixed flow reactor*. Geochimica et Cosmochimica Acta, 1990. 54(4): p. 955-969.
73. Heaney, P.J., *Structure and chemistry of the low pressure silica polymorphs*, in *Silica: Physical behavior, geochemistry, and materials applications*, P.J. Heaney,

- C.T. Prewitt, and G.V. Gibbs, Editors. 1994, Mineralogical Society of America: Washington, DC. p. 1-40.
74. Iler, R.K., *The Chemistry of Silica*. 1979, New York: Wiley- Interscience. 866.
75. Lasaga, A.C. and G.V. Gibbs, *Ab-initio quantum mechanical calculations of water-rock interactions: Adsorption and hydrolysis reactions*. American Journal of Science, 1990. 290: p. 263-295.
76. Rimstidt, J.D. and H.L. Barnes, *The kinetics of silica-water reactions*. Geochimica et Cosmochimica Acta, 1980. 44(11): p. 1683-1699.
77. Van Cappellen, P. and L. Qiu, *Biogenic silica dissolution in sediments of the Southern Ocean. II. Kinetics*. Deep Sea Research Part II: Topical Studies in Oceanography, 1997. 44(5): p. 1129-1149.
78. Renders, P.J.N., C.H. Gammons, and H.L. Barnes, *Precipitation and dissolution rate constants for cristobalite from 150 to 300[degree sign]C*. Geochimica et Cosmochimica Acta, 1995. 59(1): p. 77-85.
79. Nelson, D.M. and M.A. Brzezinski, *Diatom growth and productivity in an oligotrophic midocean gyre: A 3-yr record from the Sargasso Sea near Bermuda*. Limnology and Oceanography, 1997. 42(3): p. 473-486.
80. Koning, E., et al., *Settling, dissolution and burial of biogenic silica in the sediments off Somalia (northwestern Indian Ocean)*. Deep Sea Research Part II: Topical Studies in Oceanography, 1997. 44(6-7): p. 1341-1360.
81. Jahnke, R.A. and D.B. Jahnke, *Rates of C, N, P and Si recycling and denitrification at the US Mid-Atlantic continental slope depocenter*. Deep Sea Research Part I: Oceanographic Research Papers, 2000. 47(8): p. 1405-1428.
82. Dixit, S. and P. Van Cappellen (2003) *Predicting benthic fluxes of silicic acid from deep-sea sediments*. Journal of Geophysical Research 108, DOI: 10.1029/2002JC001309.
83. Greenwood, J.E., V.W. Truesdale, and A.R. Rendell, *Biogenic silica dissolution in seawater -- in vitro chemical kinetics*. Progress In Oceanography, 2001. 48(1): p. 1-23.
84. Hurd, D.C. and S. Birdwhistell, *On producing a more general model for biogenic silica dissolution*. American Journal of Science, 1983. 283(1): p. 1-28.
85. Kamatani, A., *Dissolution rates of silica from diatoms decomposing at various temperatures*. Marine Biology, 1982. 68(1): p. 91-96.

86. Kamatani, A., J.P. Riley, and G. Skirrow, *The dissolution of opaline silica of diatom tests in sea water*. Journal of the Oceanographical Society of Japan, 1980. 36: p. 201-8.
87. Tréguer, P., et al., *Kinetics of Dissolution of Antarctic Diatom Frustules and the Biogeochemical Cycle of Silicon in the Southern Ocean*. Polar Biology, 1988. 9(6): p. 397-403.
88. Hurd, D.C., *Factors affecting solution rate of biogenic opal in seawater*. Earth and Planetary Science Letters, 1972. 15(4): p. 411.
89. Truesdale, V., J. Greenwood, and A. Rendell, *The Rate-equation for Biogenic Silica Dissolution in Seawater – New Hypotheses*. Aquatic Geochemistry, 2005. 11(3): p. 319-343.
90. Van Cappellen, P. and L. Qiu, *Biogenic silica dissolution in sediments of the Southern Ocean. I. Solubility*. Deep Sea Research Part II: Topical Studies in Oceanography, 1997. 44(5): p. 1109-1128.
91. Gallinari, M., et al., *The importance of water column processes on the dissolution properties of biogenic silica in deep-sea sediments I. Solubility*. Geochimica et Cosmochimica Acta, 2002. 66(15): p. 2701-2717.
92. Schmidt, M., et al., *Oxygen isotopes of marine diatoms and relations to opal-A maturation*. Geochimica et Cosmochimica Acta, 2001. 65(2): p. 201-211.
93. Van Cappellen, P., *Reactive surface area control of the dissolution kinetics of biogenic silica in deep-sea sediments*. Chemical Geology, 1996. 132(1-4): p. 125-130.
94. Loucaides, S., P. Van Cappellen, and T. Behrends, *Dissolution of biogenic silica from land to ocean: The role of salinity and pH*. Limnology and Oceanography, 2008. 53: p. 1614-1621.
95. Lawson, D.S., D.C. Hurd, and H.S. Pankratz, *Silica dissolution rates of phytoplankton assemblages at various temperatures*. American Journal of Science, 1978. 278: p. 1373-1393.
96. Icenhower, J.P. and P.M. Dove, *The dissolution kinetics of amorphous silica into sodium chloride solutions: effects of temperature and ionic strength*. Geochimica et Cosmochimica Acta, 2000. 64(24): p. 4193-4203.
97. Jourabchi, P., P. Van Cappellen, and P. Regnier, *Quantitative interpretation of pH distributions in aquatic sediments: A reaction-transport modeling approach*. American Journal of Science, 2005. 305(9): p. 919-956.
98. Hurd, D.C., *Interactions of biogenic opal, sediment and seawater in the Central Equatorial Pacific*. Geochimica et Cosmochimica Acta, 1973. 37(10): p. 2257.

99. Ploug, H., et al., *Photosynthesis, respiration, and carbon turnover in sinking marine snow from surface waters of Southern California Bight: implications for the carbon cycle in the ocean*. Marine Ecology Progress Series, 1999. 179: p. 1-11.
100. Dixit, S. and P. Van Cappellen, *Surface chemistry and reactivity of biogenic silica*. Geochimica et Cosmochimica Acta, 2002. 66(14): p. 2559-2568.
101. Fraysse, F., et al., *Surface properties, solubility and dissolution kinetics of bamboo phytoliths*. Geochimica et Cosmochimica Acta, 2006. 70(8): p. 1939-1951.
102. Dove, P.M. and S.F. Elston, *Dissolution kinetics of quartz in sodium-chloride solutions - analysis of existing data and a rate model for 25-Degrees-C*. Geochimica Et Cosmochimica Acta, 1992. 56(12): p. 4147-4156.
103. Wirth, G.S. and J.M. Gieskes, *The initial kinetics of the dissolution of vitreous silica in aqueous media*. Journal of Colloid and Interface Science, 1979. 68(3): p. 492-500.
104. Fraysse, F., et al., *Aqueous reactivity of phytoliths and plant litter: Physico-chemical constraints on terrestrial biogeochemical cycle of silicon*. Journal of Geochemical Exploration, 2006. 88(1-3): p. 202-205.
105. Dove, P.M. and C.J. Nix, *The influence of the alkaline earth cations, magnesium, calcium, and barium on the dissolution kinetics of quartz*. Geochimica et Cosmochimica Acta, 1997. 61(16): p. 3329-3340.
106. Willey, J.D., *The effect of pressure on the solubility of amorphous silica in seawater at 0[deg]C*. Marine Chemistry, 1974. 2(4): p. 239.
107. Dove, P.M., *The dissolution kinetics of quartz in aqueous mixed cation solutions*. Geochimica et Cosmochimica Acta, 1999. 63(22): p. 3715-3727.
108. Kamiya, H. and K. Shimokata. *The role of salts in the dissolution of powdered quartz*. in *International symposium on Water-Rock Interactions*. 1976. Prague, Czechoslovakia: Czechoslovakian Geological Survey.
109. Van Lier, J.A., P.L. DeBruyn, and J.T.G. Overbeek, *The solubility of quartz*. Journal of Physical Chemistry, 1960. 64: p. 1675-1682.
110. Lemaire, E., et al., *Distribution of phytoplankton pigments in nine European estuaries and implications for an estuarine typology*. Biogeochemistry, 2002. 59(1): p. 5-23.
111. Ragueneau, O., et al., *Biogeochemical Transformations of Inorganic Nutrients in the Mixing Zone between the Danube River and the North-western Black Sea*. Estuarine, Coastal and Shelf Science, 2002. 54(3): p. 321-336.

112. Conley, D.J., *Riverine contribution of biogenic silica to the oceanic silica budget*. *Limnology and Oceanography*, 1997. 42(4): p. 774-777.
113. Laruelle, G.G., et al., *Anthropogenic perturbations of the silicon cycle at the global scale: Key role of the land-ocean transition*. *Global Biogeochemical Cycles*, 2009. 23(4): p. GB4031.
114. Rabouille, C., et al., *Biogenic silica recycling in surficial sediments across the Polar Front of the Southern Ocean (Indian Sector)*. *Deep Sea Research Part II: Topical Studies in Oceanography*, 1997. 44(5): p. 1151-1176.
115. Van Beusekom, J.E.E., et al., *Aluminium and silicic acid in water and sediments of the Enderby and Crozet Basins*. *Deep Sea Research Part II: Topical Studies in Oceanography*, 1997. 44(5): p. 987.
116. van der Weijden, A.J. and C.H. van der Weijden, *Silica fluxes and opal dissolution rates in the northern Arabian Sea*. *Deep Sea Research Part I: Oceanographic Research Papers*, 2002. 49(1): p. 157-173.
117. Boudreau, B.P., *Asymptotic Forms and Solutions of the Model for Silica-Opal Diagenesis in Bioturbated Sediments*. *Journal of Geophysical Research*, 1990. 95(C5): p. 7367-7379.
118. Khalil, K., et al., *Constraining biogenic silica dissolution in marine sediments: A comparison between diagenetic models and experimental dissolution rates*. *Marine Chemistry*, 2007. 106(1-2): p. 223-238.
119. King, S.L., P.N. Froelich, and R.A. Jahnke, *Early diagenesis of germanium in sediments of the Antarctic South Atlantic: in search of the missing Ge sink*. *Geochimica et Cosmochimica Acta*, 2000. 64(8): p. 1375-1390.
120. Ragueneau, O., et al., *The benthic silica cycle in the Northeast Atlantic: annual mass balance, seasonality, and importance of non-steady-state processes for the early diagenesis of biogenic opal in deep-sea sediments*. *Progress In Oceanography*, 2001. 50(1-4): p. 171-200.
121. Michalopoulos, P. and R.C. Aller, *Early diagenesis of biogenic silica in the Amazon delta: alteration, authigenic clay formation, and storage*. *Geochimica et Cosmochimica Acta*, 2004. 68(5): p. 1061-1085.
122. Presti, M. and P. Michalopoulos, *Estimating the contribution of the authigenic mineral component to the long-term reactive silica accumulation on the western shelf of the Mississippi River Delta*. *Continental Shelf Research*, 2008. 28(6): p. 823-838.
123. Van Bennekom, A.J., et al., *Aluminium-rich opal: an intermediate in the preservation of biogenic silica in the Zaire (Congo) deep-sea fan*. *Deep Sea Research Part A. Oceanographic Research Papers*, 1989. 36(2): p. 173-190.

124. Gehlen, M., et al., *Unraveling the atomic structure of biogenic silica: evidence of the structural association of Al and Si in diatom frustules*. *Geochimica et Cosmochimica Acta*, 2002. 66(9): p. 1601-1609.
125. Koning, E., et al., *Rapid post-mortem incorporation of aluminum in diatom frustules: Evidence from chemical and structural analyses*. *Marine Chemistry*, 2007. 106(1): p. 97-111.
126. DeMaster, D.J., *The accumulation and cycling of biogenic silica in the Southern Ocean: revisiting the marine silica budget*. *Deep Sea Research Part II: Topical Studies in Oceanography*, 2002. 49(16): p. 3155-3167.
127. Mackenzie, F.T. and R.M. Garrels, *Chemical mass balance between rivers and oceans*. *American Journal of Science*, 1966. 264(7): p. 507-525.
128. Michalopoulos, P., R.C. Aller, and R.J. Reeder, *Conversion of diatoms to clays during early diagenesis in tropical, continental shelf muds*. *Geology*, 2000. 28(12): p. 1095-1098.
129. Loucaides, S., et al., *Seawater-mediated interactions between diatomaceous silica and terrigenous sediments: Results from long-term incubation experiments*. *Chemical Geology*, 2010. 270(1-4): p. 68-79.
130. Hurd, D.C. and F. Theyer, *Changes in physical and chemical properties of biogenic silica from the Central Equatorial Pacific. I. Solubility, specific surface area, and solution rate constants of acid-cleaned samples*, in *Analytical Methods in Oceanography*, T.R.P.J. Gibb, Editor. 1974, American Chemical Society: Washington D. C. p. 211-230.
131. Gendron-Badou, A., et al., *Spectroscopic characterization of biogenic silica*. *Journal of Non-Crystalline Solids*, 2003. 316(2-3): p. 331-337.